DOI 10.1007/s11141-018-9912-5
Radiophysics and Quantum Electronics, Vol. 61, No. 7, December, 2018
(Russian Original Vol. 61, No. 7, July, 2018)

SCATTERING OF A PLANE ELECTROMAGNETIC WAVE BY A MULTILAYER SPHERICAL LENS

P. O. Afanasyev,[1] A. A. Akopov,[2] A. M. Lehrer,[2] and M. B. Manuilov[3*]

UDC 621.396.67

We propose an analytical solution of the problem of diffraction of a plane electromagnetic wave by a multilayer dielectric (including plasmon) sphere. The solution is obtained using the method of separation of variables. New efficient recurrence relationships are obtained for calculations of the fields in layers, as well as formulas for the fields in the near and far diffraction zones. The novelty of the proposed solution is connected with the way of representing its radial part in the form of normalized functions. It is shown that as the number of the lens layers, which approximate the smooth profile of dielectric permittivity, grows, the electric field at the focusing point increases and reaches the maximum value. This allows one to determine the minimum required number of layers in practical problems. Resonance properties of metal-dielectric nanoparticles are studied in the optical band.

1. INTRODUCTION

Currently, multibeam antennas are used increasingly frequently as base station antennas to enhance the bandwidth capacity of mobile communication systems in locations with great numbers of subscribers. In this case, the service sector is covered by several narrow beams, each of which corresponds to its own base station. From this viewpoint, multibeam antennas based on multilayer Luneberg lenses [1, 2] proved to offer a promising solution. Due to their spherical symmetry, such lenses can form several independent radiation patterns in a significantly wider range of angles compared to other antenna types known. Then, along with the high velocity of beam switching and the low level of side lobes, a high level of the channel isolation is ensured. Additionally, spherical symmetry makes it possible to tilt the beam without turning the entire antenna and almost with no radiation pattern distortions.

Despite the above-listed advantages, Luneberg lenses have been of limited use in antenna engineering so far due to technological complexity of manufacturing dielectric structures with the radial dependence of dielectric permittivity. Recently, due to the arrival of novel types of electromagnetic materials with preset parameters, a possibility has appeared to create multilayer structures, in which the distribution of the dielectric permittivity of a Luneberg lens is realized with acceptable accuracy. Technologies of manufacturing gradient lenses, in which the required dependence of the refractive index on the radius is formed, have also been developed [3].

In this connection, it is important to have adequate means and methods for modeling the diffraction of electromagnetic waves by a layered inhomogeneous dielectric sphere. The methods of solving this problem were reviewed most comprehensively in [4].

* m_manuilov@sfedu.ru

[1] National University of Ireland, Maynooth, Ireland; [2] Rostov-on-Don Research Institute of Radiocommunications, Rostov-on-Don; [3] Southern Federal University, Rostov-on-Don, Russia. Translated from Izvestiya Vysshikh Uchebnykh Zavedenii, Radiofizika, Vol. 61, No. 7, pp. 583–595, July 2018. Original article submitted May 25, 2018; accepted July 26, 2018.

Geometrical optics methods are widely used to analyze spherical lens antennas, as well as lens antennas of other types [3, 5–13]. It is usually assumed that a lens is irradiated by a point source located at a certain distance from its surface. This approach yields acceptable results in cases where the lens size is much greater than the radiation wavelength. To overcome this limitation, the ray tracing method was combined with the diffraction theory in [14], and the combined method of ray tracing and physical optics was used in [15] to analyze double-layer Luneberg lenses. All the above-mentioned methods do not allow for rereflections at the layer boundaries, which reduces the calculation accuracy.

For layered spherical structures, the homogeneous Helmholtz equation can be solved by numerical-analytical methods. The general scheme of solving the electrodynamic problem for a layered Luneberg lens [16] consists in solving the system of linear equations, which follow from the conditions of continuity of the tangential components in the electric-field and magnetic-field vectors at the layer interfaces. In this case, the order of the system is determined by the number of layers. The amplitudes of the fields in the layers are found by solving this system. Then the field in the outer region is determined, and from it, the antenna radiation characteristics are found.

The literature on the problem of diffraction of a plane wave by spherically shaped bodies is quite extensive [17, 18]. For the first time, it was solved by G. Mie [19]. Mie's theory was described comprehensively in [20]. Independently of Mie's work, an equivalent solution of this problem was obtained by Debye in his work on light pressure [21]. In both cases, the electric and magnetic fields are represented as series. The total field outside the sphere is expressed in the form of the sum of the incident and scattered fields. The diffraction problem is solved basing on the conditions of continuity of the field components at the interfaces of dielectric layers.

Later, the Mie solution was generalized to the case of diffraction of a plane wave by a radially inhomogeneous sphere. The problems of diffraction of a plane wave by a double-layer sphere and a dielectric body consisting of an arbitrary number of concentric layers were solved in [22] and [23], respectively. An improved method of solving the diffraction problem was proposed in [24] and modified in [4], where the authors managed to avoid complex calculations of logarithmic derivatives.

The Mie series expansion was first used to solve the problem of scattering of a plane electromagnetic wave by a conducting sphere [25], and then, by a dielectric sphere [26]. Afterwards, the problem of wave scattering by a layered dielectric structure was solved in different ways: by using the Mie series [27, 28], the scalar potentials [29], the Green's tensor functions [30, 31], and the mode matching methods [32, 33]. In doing this, the antenna characteristics of the Luneberg lens were studied for the case of irradiation from real sources [33, 34]. In [35], the two-dimensional model of such a lens was considered. In [36], the analytical solution on integral equations for the Debye potentials was obtained for the case of a homogeneous or layered sphere.

Currently, numerical methods are used increasingly frequently to analyze Luneberg lenses, such as the finite-difference time domain method [37], the finite element method [38], and the method of moments [39, 40]. An advantage of these methods is their universality and calculation flexibility. This makes it possible, e.g., to allow for the antenna characteristics of various structural elements. A drawback of such methods is that they require sufficiently great computational resources, and the computation time increases strongly as the electric dimensions grow.

The classical Luneberg lens converts a plane electromagnetic wave to a spherical one, and vice versa. To study the focusing properties of a multilayer Luneberg lens as a function of the number of layers, one should consider the problem of plane wave diffraction by such a lens. This problem can be solved by both the numerical methods, which are implemented in the electrodynamic modeling software suites, and by analytical ones. However, in the case of great geometric sizes of the lens the numerical solution of the diffraction problem can require significant computational resources.

In what follows, we present a new effective analytical solution of the problem of plane wave diffraction by a multilayer dielectric sphere. On the one hand, high numerical efficiency and good accuracy of the proposed solution allow one to use it as the computational kernel for synthesis of the dielectric-permittivity

profile of a multilayer lens with complex dielectric permittivities of the layers. On the other hand, this solution can be regarded as a reference for testing of universal numerical methods.

Additionally, in this paper we study theoretically the resonance properties of spherical metal-dielectric particles in the optical range. When in resonance, the amplitude of the electromagnetic field near a nanoparticle increases by more than an order of magnitude as compared with the amplitude of the incident-wave field. This effect is used in sensors, biodetectors, elements of optical integral circuits, fluorescent microscopy, and nonlinear spectroscopy [41]. Most papers deal with studying the influence of the dimensions of metal nanoparticles on the resonance properties of the particles. Some aspects of the influence of the sizes and shapes of the particles on their scattering properties are studied, specifically, on the extinction cross section and the scattered field [42, 43]. In this paper, we study the properties of spherical metal-dielectric parties, which are coated with a dielectric sheath. The limits of applicability of the quasistatic approximation [41] in the calculations of metal-dielectric nanostructures are estimated.

2. SOLUTION METHOD

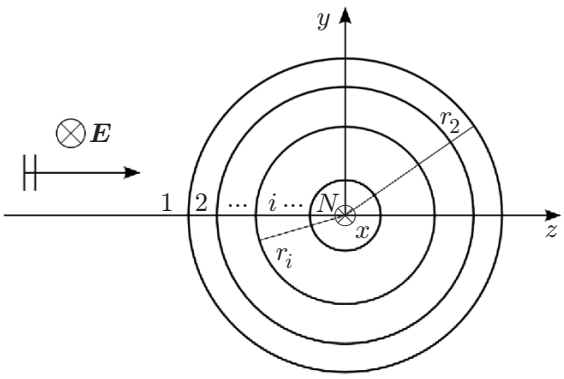

Fig. 1. Formulation of the problem of diffraction of a plane wave by a multilayer dielectric sphere.

Consider scattering of a plane electromagnetic wave by a dielectric sphere which consists of N homogeneous concentric layers. The sphere is located in a medium with the dielectric permittivity ε_1 and magnetic permeability μ_1, see Fig. 1. The layers are numbered from the outer layer towards the inner one. The permittivity and permeability of the layers are ε_i and μ_i, respectively, and the layer radii are r_i, where $i = 2, 3, \ldots, N$. The incident plane wave is linearly polarized, the electric-field vector is directed along the x axis, and the direction of its propagation coincides with the z axis.

To solve the problem of the plane wave diffraction by a multilayer sphere, we will use a representation of the components of the field of this wave in terms of the Debye potentials [18], specifically, A (electric potential) and F (magnetic potential). For the electric waves ($H_r = 0$), the components of the electric and magnetic fields ($\mathbf{E}$ and $\mathbf{H}$, respectively) are expressed through the electric Debye potential as follows:

$$E_\varphi = \frac{1}{r\sin\theta}\frac{\partial^2(rA)}{\partial r\partial\varphi}, \qquad E_\theta = \frac{1}{r}\frac{\partial^2(rA)}{\partial r\partial\theta}, \qquad E_r = \frac{\partial^2(rA)}{\partial r^2} + k^2 rA,$$

$$H_\theta = i\omega\varepsilon\varepsilon_0\frac{1}{r\sin\theta}\frac{\partial(rA)}{\partial\varphi}, \qquad H_\varphi = -i\omega\varepsilon\varepsilon_0\frac{1}{r}\frac{\partial(rA)}{\partial\theta}, \tag{1}$$

where ε_0 is the electric constant, ω is the angular frequency of the radiation, and k and ε are the wave number and the dielectric permittivity at the point having the spherical coordinates r, θ, φ, respectively.

The wave equation, which the electric Debye potential should satisfy, has the form

$$\frac{\partial^2(rA)}{\partial r^2} + \frac{1}{r^2\sin\theta}\left[\frac{1}{\sin\theta}\frac{\partial^2(rA)}{\partial\varphi^2} + \frac{\partial}{\partial\theta}\frac{\partial(rA\sin\theta)}{\partial\theta}\right] + k^2 rA = 0.$$

Note that the conditions of continuity of the tangential field components at the layer boundaries lead to the continuity of the values εA and $\partial(rA)/\partial r$.

For the magnetic waves ($E_r = 0$), the field components are expressed in terms of the magnetic Debye potential:

$$E_\theta = -i\omega\mu\mu_0\frac{1}{r\sin\theta}\frac{\partial(rF)}{\partial\varphi}, \qquad E_\varphi = i\omega\mu\mu_0\frac{1}{r}\frac{\partial(rF)}{\partial\theta},$$

$$H_\varphi = \frac{1}{r\sin\theta}\frac{\partial^2(rF)}{\partial r\partial\varphi}, \qquad H_\theta = \frac{1}{r}\frac{\partial^2(rF)}{\partial r\partial\theta}, \qquad H_r = \frac{\partial^2(rF)}{\partial r^2} + k^2 rF, \tag{2}$$

where μ_0 is the magnetic constant, and μ is the magnetic permeability at the point having the spherical coordinates r, θ, φ. The potential F satisfies the same wave equation and conditions of continuity of the values μF and $\partial(rF)/\partial r$ at the layer boundaries.

The solutions of the wave equations will be sought for, as usual, by the method of separation of variables [18]. We assume that a magnetic wall is located in the plane $y = 0$. In the pth layer of the considered structure, the solution will be written in the following form [18]:

$$A_p(r,\theta,\varphi) = \sum_{m=0}^{\infty}\sum_{n=1}^{\infty} a_{p,n,m} R^a_{p,n}(r) P^m_n(\cos\theta)\cos(m\varphi), \tag{3}$$

$$F_p(r,\theta,\varphi) = \sum_{m=1}^{\infty}\sum_{n=1}^{\infty} f_{p,n,m} R^f_{p,n}(r) P^m_n(\cos\theta)\sin(m\varphi), \tag{4}$$

where $a_{p,n,m}$ and $f_{p,n,m}$ are unknown coefficients, and $P^m_n(z)$ is the associated Legendre functions. The functions $R^\sigma_{p,n}(r)$ in Eqs. (3) and (4) are the solution of the equation

$$\frac{\mathrm{d}^2[rR^\sigma_{p,n}(r)]}{\mathrm{d}r^2} + \left[k_p^2 - \frac{n\,(n+1)}{r^2}\right] rR^\sigma_{p,n}(r) = 0, \tag{5}$$

where $\sigma = a, f$, and $k_p = \omega\sqrt{\varepsilon_p\varepsilon_0\mu\mu_0}$ is the wave number in the pth layer. In this case, the conditions of continuity at the layer interfaces inside the sphere should be fulfilled for the functions

$$\varepsilon_p R^a_{p,n}(r), \quad \frac{\mathrm{d}[rR^a_{p,n}(r)]}{\mathrm{d}r}, \quad \mu_p R^f_{p,n}(r), \quad \frac{\mathrm{d}[rR^f_{p,n}(r)]}{\mathrm{d}r}.$$

To simplify further calculations, we will require that the functions $R^\sigma_{1,n}(r)$ and $R^\sigma_{2,n}(r)$ from Eq. (5) should satisfy the conditions of normalization at the outer boundary of the sphere:

$$R^\sigma_{1,n}(r_2) = R^\sigma_{2,n}(r_2) = 1. \tag{6}$$

The solution of wave equation (5) is expressed in terms of spherical Bessel functions. For the external region ($p = 1$), it has the form $R^\sigma_{1,n}(r) = h_n(k_1 r)/h_n(k_1 r_2)$, where $h_n(z) = \sqrt{\pi/(2z)}H^{(2)}_{n+1/2}(z) = j_n(z) - iy_n(z)$ is a spherical Hankel function of the second kind, and $j_n(z)$ and $y_n(z)$ are spherical Bessel functions of the first and second kinds, respectively.

Let us represent the field outside the sphere as a sum of the field of the incident wave and the scattered field. For the field of the incident wave, the Debye potentials can be represented as the following series:

$$A^{\mathrm{inc}}(r,\theta,\varphi) = \sum_{n=1}^{\infty} a^{\mathrm{inc}}_n \frac{j_n(k_1 r)}{j_n(k_1 r_2)} P^m_n(\cos\theta)\cos\varphi, \tag{7}$$

$$F^{\mathrm{inc}}(r,\theta,\varphi) = \sum_{n=1}^{\infty} f^{\mathrm{inc}}_n \frac{j_n(k_1 r)}{j_n(k_1 r_2)} P^m_n(\cos\theta)\sin\varphi. \tag{8}$$

In the spherical coordinate system, the components of the electric field of the incident plane wave, which is polarized along the x axis, will have the form

$$E^{\mathrm{inc}}_r = E\sin\theta\cos\varphi, \qquad E^{\mathrm{inc}}_\theta = E\cos\theta\cos\varphi, \qquad E^{\mathrm{inc}}_\varphi = -E\sin\varphi,$$
$$E = \exp(-ik_1 r_2\cos\theta)\sin\theta\cos\varphi. \tag{9}$$

One can see from relationship (9) that it is necessary to set $m = 1$, i.e., the other terms of the series are equal to zero. Using the table series expansion [18], we find the coefficients in series (7) and (8):

$$a_n^{\text{inc}} = \frac{1}{k_1} j_n(k_1 r_2) \frac{2n+1}{n\,(n+1)} (-i)^{n-1}, \qquad f_n^{\text{inc}} = \frac{1}{Z_{c,1} k_1} j_n(k_1 r_2) \frac{2n+1}{n\,(n+1)} (-i)^{n-1},$$

where $Z_{c,\,1}$ is the wave impedance of the region outside the sphere. Then, using the conditions of continuity of the Debye potentials and their derivatives on the sphere surface, we find the unknown coefficients in expansions (3) and (4) for $p = 1$:

$$a_{1,n} = \frac{\varepsilon_1 \dot{R}^a_{2,n}(r_2) - \varepsilon_2 k_1 j_n'(k_1 r_2)/j_n(k_1 r_2)}{\Delta_a} a_n^{\text{inc}}, \quad a_{2,n} = \varepsilon_1 \frac{\dot{R}^a_{1,n}(r_2) - k_1 j_n'(k_1 r_2)/j_n(k_1 r_2)}{\Delta_a} a_n^{\text{inc}}, \tag{10}$$

$$f_{1,n} = \frac{\mu_1 \dot{R}^f_{2,n}(r_2) - \mu_2 k_1 j_n'(k_1 r_2)/j_n(k_1 r_2)}{\Delta_f} f_n^{\text{inc}}, \quad f_{2,n} = \mu_1 \frac{\dot{R}^f_{1,n}(r_2) - k_1 j_n'(k_1 r_2)/j_n(k_1 r_2)}{\Delta_f} f_n^{\text{inc}}, \tag{11}$$

where $\Delta_a = \varepsilon_2 R^a_{1,n}(r_2) - \varepsilon_1 \dot{R}^a_{2,n}(r_2)$, $\Delta_f = \mu_2 \dot{R}^f_{1,n}(r_2) - \mu_1 \dot{R}^f_{2,n}(r_2)$, the prime superscript denotes the derivative with respect to the argument, and the dot over a variable denotes the differentiation operator here and in what follows: $\dot{R} \equiv \mathrm{d}[rR(r)]/\mathrm{d}r$.

Thus, the electric and magnetic Debye potentials for the scattered field in the outer region ($p = 1$) are expressed in the form of series

$$A_1(r,\theta,\varphi) = \sum_{n=1}^{\infty} a_{1,n} R^a_{1,n}(r) P_n^1(\cos\theta)\cos\varphi = \sum_{n=1}^{\infty} a_{1,n} \frac{h_n(k_1 r)}{h_n(k_1 r_2)} P_n^1(\cos\theta)\cos\varphi, \tag{12}$$

$$F_1(r,\theta,\varphi) = \sum_{n=1}^{\infty} f_{1,n} R^f_{1,n}(r) P_n^1(\cos\theta)\cos\varphi = \sum_{n=1}^{\infty} f_{1,n} \frac{h_n(k_1 r)}{h_n(k_1 r_2)} P_n^m(\cos\theta)\cos\varphi. \tag{13}$$

The components of the electric fields can be expressed in terms of the Debye potentials allowing for Eqs. (1) and (2) as follows:

$$E_\varphi = \frac{1}{r\sin\theta} \frac{\partial^2 (rA)}{\partial r \partial \varphi} + i\omega\mu\mu_0 \frac{1}{r} \frac{\partial (rF)}{\partial \theta}, \qquad E_\theta = \frac{1}{r} \frac{\partial^2 (rA)}{\partial r \partial \theta} - i\omega\mu\mu_0 \frac{1}{r\sin\theta} \frac{\partial (rF)}{\partial \varphi}. \tag{14}$$

To determine the field inside the sphere, one has to find the functions $R^a_{p,n}(r)$ and $R^f_{p,n}(r)$ in expressions (3) and (4) at $p = 2, \ldots, N$ and satisfy the conditions of continuity for these functions and their derivatives.

We will look for the solution in the form

$$R^a_{p,n}(r) = \begin{cases} \dfrac{K_N}{\varepsilon_N} \dfrac{j_n(k_N r)}{j_n(k_N r_N)} = \dfrac{K_N}{\varepsilon_N} \Phi^-_{N,n}(r), & p = N, \quad 0 \le r \le r_N; \\ \dfrac{1}{\varepsilon_p} [K_p \Phi^-_{p,n}(r) + K_{p+1} \Phi^+_{p,n}(r)], & 2 < p < N, \quad r_{p+1} \le r \le r_p, \end{cases} \tag{15}$$

where K_p denotes unknown coefficients, and $\Phi^+_{p,n}(r)$ and $\Phi^-_{p,n}(r)$ are the functions that satisfy Eq. (5) and the boundary conditions

$$\Phi^-_{p,n}(r_p) = 1, \quad \Phi^+_{p,n}(r_p) = 0, \quad \Phi^-_{p,n}(r_{p+1}) = 0, \quad \Phi^+_{p,n}(r_{p+1}) = 1, \quad \Phi^+_{N,n}(r_p) = 0. \tag{16}$$

Functions (15) that are introduced here satisfy the conditions of continuity of the quantity $\varepsilon_p R^a_{p,n}(r)$ at $r = r_{p+1}$, $p = 2, \ldots, N-1$. This simplifies writing of the continuity conditions for the derivatives $\mathrm{d}[rR^a_{p,n}(r)]/\mathrm{d}r$ at the layer boundaries at $r = r_{p+1}$, $p = 2, \ldots, N-1$ considerably. At the same time, in literature, e.g., in [4, 32], a representation of the solution in the layers is used in the form of a linear

combination of the spherical Bessel functions of the first and second kinds, which leads to significantly more complicated transformations and resulting relationships. From the condition of continuity of the derivatives $\mathrm{d}[rR^a_{p,n}(r)]/\mathrm{d}r$ at the layer interfaces and $r = r_{p+1}$, $p = 2, \ldots, N-1$, using representation (15) we obtain

$$K_p \frac{1}{\varepsilon_p} \dot{\Phi}^-_{p,n}(r_{p+1}) + K_{p+1} \left[\frac{1}{\varepsilon_p} \dot{\Phi}^+_{p,n}(r_{p+1}) - \frac{1}{\varepsilon_{p+1}} \dot{\Phi}^-_{p+1,n}(r_{p+1}) \right] = K_{p+2} \frac{1}{\varepsilon_{p+1}} \dot{\Phi}^+_{p+1,n}(r_{p+1}), \tag{17}$$

$p = N-1, \ldots, 2$. From normalization conditions (6), it follows that

$$R^a_{2,n}(r_2) = K_2/\varepsilon_2 = 1. \tag{18}$$

Relationships (17) and (18) are a recurrence scheme for determination of the unknown coefficients K_p. Calculating these coefficients, we find the function $R^a_{2,n}(r)$, which is required to satisfy the boundary condition on the sphere surface:

$$R^a_{2,n}(r) = \frac{1}{\varepsilon_2} [K_2 \Phi^-_{2,n}(r) + K_3 \Phi^+_{2,n}(r)]. \tag{19}$$

To determine the function $R^f_{p,n}(r_2)$, one should replace ε in Eqs. (17)–(19) with μ.

The functions $\Phi^+_{p,n}(r)$ and $\Phi^-_{p,n}(r)$, which enter Eqs. (15)–(17) and satisfy boundary conditions (16), can be represented as

$$\Phi^+_{p,n}(r) = \frac{1}{\delta} [j_n(k_p r) y_n(k_p r_p) - j_n(k_p r_p) y_n(k_p r)], \; \Phi^-_{p,n}(r) = \frac{1}{\delta} [j_n(k_p r) y_n(k_p r_{p+1}) - j_n(k_p r_{p+1}) y_n(k_p r)],$$

where $\delta = j_n(k_p r_p) y_n(k_p r_{p+1}) - j_n(k_p r_{p+1}) y_n(k_p r_p)$.

After calculating the functions $R^a_{p,n}(r)$ and $R^f_{p,n}(r)$ in Eq. (15), it is possible to determine the coefficients $a_{1,n}$ and $f_{1,n}$ from Eqs. (10) and (11). Substituting these coefficients to series (12) and (13), we determine the Debye potentials of the scattered field in the outer region by using relationships (14).

Allowing for the asymptotic behavior of the Bessel functions at great values of the argument, one can show that within the far-zone approximation ($k_1 r \to \infty$), the expressions for the Debye potentials and the derivatives take the form

$$A_1(r,\theta,\varphi) \sim \frac{1}{k_1 r} \sum_{n=1}^{\infty} a_{1,n} \frac{\exp\{-i\,[k_1 r - \pi\,(n+1)/2]\}}{h_n(k_1 r_2)} P^1_n(\cos\theta) \cos\varphi,$$

$$\frac{\partial A_1(r,\theta,\varphi)}{\partial r} \sim -ik_1 A_1(r,\theta,\varphi),$$

$$F_1(r,\theta,\varphi) \sim \frac{1}{k_1 r} \sum_{n=1}^{\infty} f_{1,n} \frac{\exp\{-i\,[k_1 r - \pi\,(n+1)/2]\}}{h_n(k_1 r_2)} P^1_n(\cos\theta) \sin\varphi,$$

$$\frac{\partial F_1(r,\theta,\varphi)}{\partial r} \sim -ik_1 F_1(r,\theta,\varphi).$$

Then the components of the electric field in the far zone are determined by the formulas

$$E_\varphi \sim ik_1 \left(-\frac{1}{\sin\theta} \frac{\partial A}{\partial \varphi} + \frac{1}{Z_{c,1}} \frac{\partial F}{\partial \theta} \right), \qquad E_\theta \sim -ik_1 \left(\frac{\partial A}{\partial \theta} + \frac{1}{Z_{c,1}} \frac{1}{\sin\theta} \frac{\partial F}{\partial \varphi} \right).$$

3. NUMERICAL RESULTS

The proposed analytical method is characterized by fast convergence with regard to the number of considered terms in the series. In the process of actual calculations, this number varied in the range from 40 to 60. The convergence rate decreases as the electrical size of the calculated structure grows. Therefore, as the lens radius grows as compared with the operating wavelength, the number of terms in expansions (12)

and (13) should be increased. Specifically, for an eight-layer lens, which is considered below, one should allow for 45 terms when summing the series, in order to achieve an error of the order of hundredths of a percent.

The advantage and efficiency of the proposed method are determined by the simple and fast recurrence scheme, which is operable at an arbitrary number of dielectric layers having complex dielectric permittivities. In this case, the computation time per frequency point is equal to less than one second for a modern PC, which is several orders of magnitude shorter than the computation times of the known off-the-shelf codes implementing the universal numerical electrodynamic methods.

To check the above-described analytical method, we studied the scattered field for the cases of incidence of a plane wave having the frequency $f_0 = 2$ GHz on a single-layer, a double-layer, or a triple-layer dielectric sphere. The radii of the layers in the triple-layer sphere were equal to 150, 200, and 250 mm, and their dielectric permittivities, to 1.77, 1.50, and 1.40, respectively. All dielectric materials had a magnetic permeability of 1 and no losses.

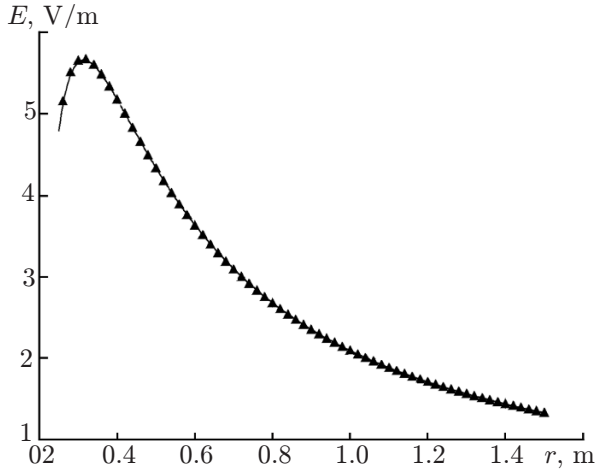

Fig. 2. Radial dependence of the electric field of the wave scattered by a three-layer sphere (r counted in the direction opposite to the wave propagation), $r_2 = 250$ mm, $r_3 = 200$ mm, $r_4 = 150$ mm, $\varepsilon_2 = 1.4$, $\varepsilon_3 = 1.5$, $\varepsilon_4 = 1.77$, $f_0 = 2$ GHz, the ▲ symbols correspond to [44], and the solid line, to the considered method.

The same problems were solved by the numerical methods implemented in the software suite in [44]. In that case, the finite elements method was used to calculate the diffraction by the single-layer sphere, and the method of moments, the diffraction by multiple-layer spheres. Figure 2 shows the calculated amplitude of the scattered electric field in the outer region. Here and in what follows, the amplitude of the incident field is equal to 1 V/m. The radial dependence of the field was calculated in the direction of the wave propagation. The dependences of the scattered-field amplitude on the angular coordinates in the E and H planes were also calculated. Graphical coincidence of the results, which were obtained by the presented analytical method and the numerical methods, is observed in all cases,

Note that the proposed solution allows one also to analyze metal-dielectric structures, e.g., nanoparticles of gold or silver coated with dielectric sheaths in the optical spectrum. In the process of the calculations, allowance was made for the dependence of the refractive indices of metals on the wavelength. The complex refractive indices of silver, gold, copper and aluminum are taken from [45].

To determine the minimal number of the layers required for focusing of a parallel beam, diffraction of a plane wave by a dielectric multilayer sphere was needed for various layer numbers that approximate the required smooth profile of the dielectric permittivity. The specified profile of the dielectric permittivity was determined by formula [9], which is a generalization of the Luneberg formula for geometric optics:

$$\varepsilon(r) = \frac{1}{\bar{F}^2}\left[1 + \bar{F}^2 - \left(\frac{r}{R}\right)^2\right], \tag{20}$$

where $R = r_2$ is the outer lens radius, $\bar{F} = R_F/R$ is the focal distance normalized with respect to the lens radius, and R_F is the distance between the lens center and the focal point.

Figures 3 and 4 show the amplitudes of the electric field scattered by an eight-layer dielectric lens ($\bar{F} = 1.1$) as functions of the radial and angular coordinates.

The radii of the layers in this sphere are equal to 112.5, 225.0, 337.5, 450.0, 562.5, 675.0, 787.5, and 900.0 mm, and the dielectric permittivities of the layers, to 1.82, 1.79, 1.74, 1.66, 1.56, 1.43, 1.27, and 1.09 (see Fig. 1). The frequency is $f_0 = 2$ GHz. The presented dependences show that the structure has a

pronounced focus situated at a distance of about 1 m from the lens center, where the electric field exceeds the amplitude of the incident wave by more than an order of magnitude. The field decreases fast as the distance from the focus grows along both the radial and angular coordinates. The calculated focal distance corresponds to the value $\bar{F} = 1.1$, which was taken in Eq. (20).

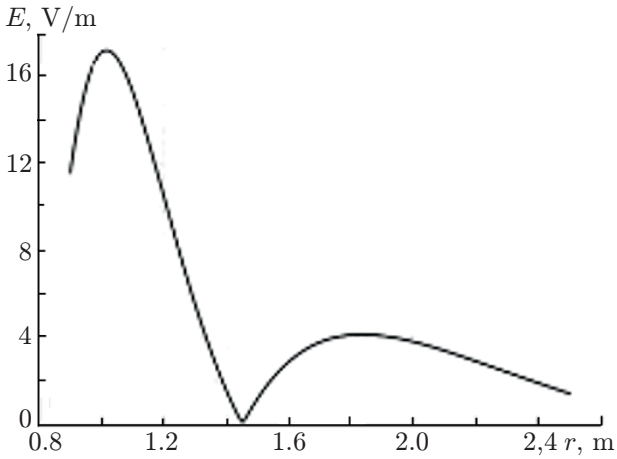

Fig. 3. Radial dependence of the electric field of a wave scattered by an eight-layer sphere (r is counted along the direction of the wave propagation).

The dependences of the electric field at the maximum of its distribution (focus) on the number of layers were studied for various frequencies of the incident wave and a structure with $\bar{F} = 1.1$ and $R = 900$ mm. In this case, the profile of the dielectric permittivity of the lens was approximated with homogeneous layers having identical thicknesses, i.e., for the number N of layers, the thickness of each layer was equal to $\Delta r = R/N$. It was found that as the number of the layers, which approximate the profile of the dielectric permittivity of the lens, increases, the electric field E at the focusing point is growing nonlinearly and, starting at a certain value, remains nearly constant. In this case, the dependence of E at the maximum of its distribution on the number of layers grows with increasing operating frequency. For example, for a lens working in two standard mobile communication bands (690–960 MHz and 1710–2690 MHz), the strongest dependence is observed for a frequency of 2690 MHz. For actual problems in the specified bands, it suffices to take $N = 8$, since at this value the maximum field is close to the limiting value.

It should be noted that the optimal number of layers is determined by not only the electric size of the lens, but also the technology of its manufacture. Whenever a technology, which allows one to produce layers with arbitrary radii, is available, the number of layers can be decreased [46].

Let us consider the resonance properties of spherical metal-dielectric nanoparticles. The calculation of the diffraction by nanoparticles has its specific features. Unlike the size of the Luneberg lens, the sizes of nanoparticles are smaller than or comparable with the wavelength. This allows one to use the obtained formula in the case of a small number of series terms. However, in this case the real and imaginary parts of the dielectric permittivity have the same order of magnitude. This required developing special procedures for calculation of the Bessel functions of the complex argument.

It is known [41] that the quasistatic approximation, within which the resonance wavelength is independent of the sphere diameter, but is determined rather by the dielectric permittivity of the particle

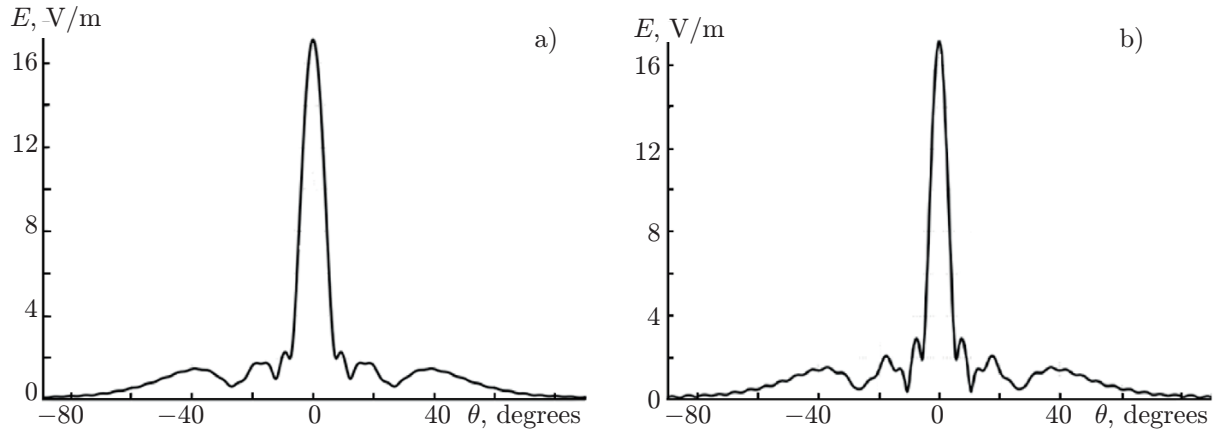

Fig. 4. Angular distribution of the electric field of the wave scattered by an eight-layer sphere in the planes of the **E** and **H** vectors (*a* and *b*, respectively). The value of r corresponds to the position of the maximum of E.

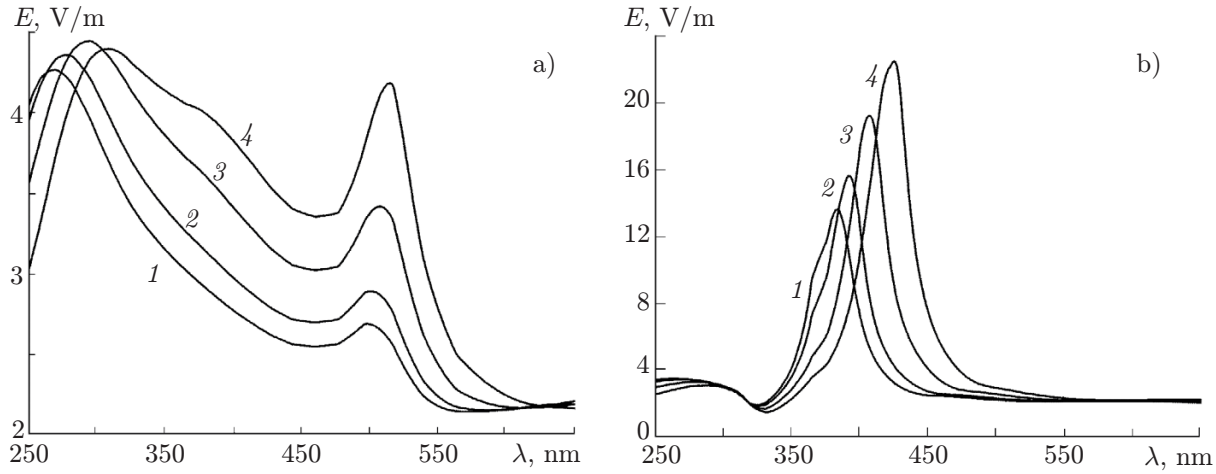

Fig. 5. Dependence of the electric field on the wavelength λ for golden (*a*) and silver (*b*) spheres, which have radii of 150 nm and are coated with sheaths having outer radii of 200 nm and $\varepsilon = 1.5$ (curve *1*), $\varepsilon = 1.6$ (*2*), $\varepsilon = 1.8$ (*3*), and $\varepsilon = 2.0$ (*4*). The distance from the sphere center is equal to 300 nm (in the direction of the wave propagation).

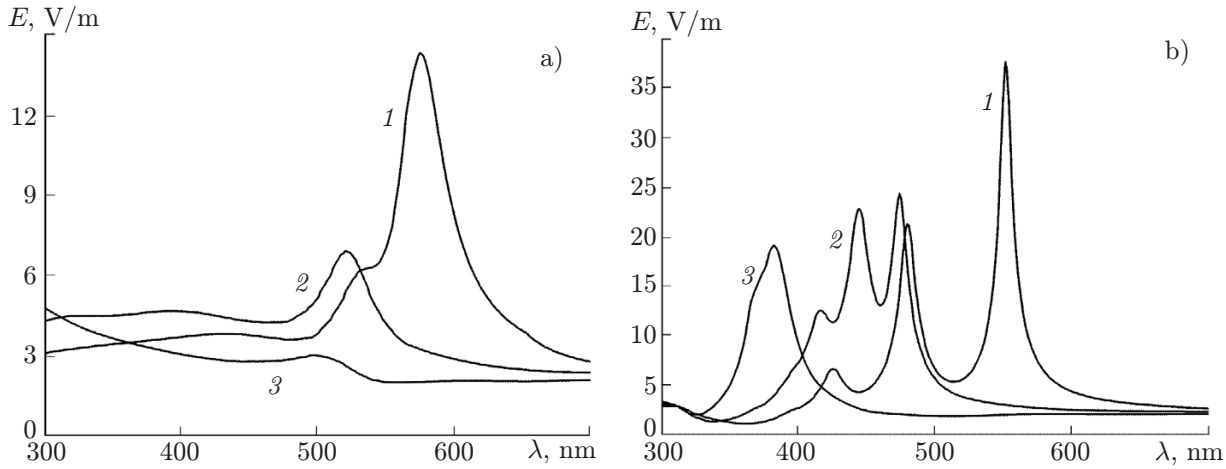

Fig. 6. Dependence of the electric field on the wavelength for gold (*a*) and silver (*b*) spheres having radii of 150 nm, 175 nm, and 200 nm (curves *1*, *2*, and *3*, respectively), which are coated in dielectric sheaths having the dielectric permittivity $\varepsilon = 1.5$. The outer radius of the spheres is equal to 250 nm. The distance from the sphere center is 300 nm (in the direction of the wave propagation).

and its surroundings, is valid for nanoparticles that have sizes much smaller than the wavelength in free space. Numerical experiments showed that the quasistatic approximation makes it possible to estimate the resonance properties with an error of less than 4% for the ratio between the particle size and the wavelength being not more than 5%.

Figures 5–7 present the results of calculating the total electric field for the diffraction of a plane wave by nanoparticles of gold and silver. An increase in the dielectric permittivity of the sheath around a plasmon nanoparticle leads to a frequency drift of the scattering maximum. A variation in the dielectric permittivity of the sheath from 1.5 to 2.0 results in an increase of the maximum total (scattered plus incident) field by about 1.8 times (see Fig. 5). A similar effect is observed, when the sheath thickness increases (see Fig. 6).

Figure 7 presents the dependences of the field on the wavelength for a triple-layer structure. As the dielectric permittivity of the outer layer changes from 1.6 to 2.0, the maximum total field increases by about 1.5 times. The resonance wavelength also increases in the case under consideration. It should be noted that it is simpler to achieve the required resonance properties in structures with a greater number of layers, since variations in one of the layers have less influence on the total characteristic.

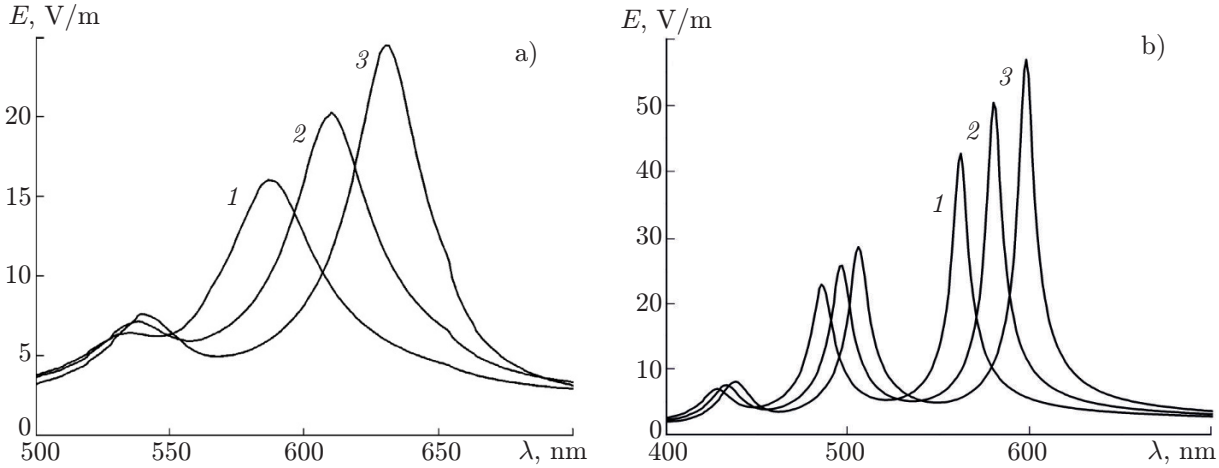

Fig. 7. Dependence of the electric field on the wavelength for gold (*a*) and silver (*b*) spheres having radii of 150 nm, 175 nm, and 200 nm (curves *1*, *2*, and *3*, respectively), which are coated in two dielectric sheaths. The radius and the dielectric permittivity of the inner sheath are equal to 200 nm and $\varepsilon = 1.5$, respectively. The outer radius is equal to 250 nm, and the dielectric permittivities are $\varepsilon = 1.6$, 1.8, and 2.0 (curves *1*, *2*, and *3*, respectively.) The distance from the sphere center is 300 nm (in the direction of the wave propagation).

4. CONCLUSIONS

We have obtained an analytical solution of the problem of diffraction of a plane electromagnetic wave by a multilayer dielectric sphere with an arbitrary number of dielectric layers having arbitrary radii and dielectric permittivity values. The solution is found by the method of separation of variables. We used representations of the fields in the layers in terms of the Debye potentials, which are written in the form of series with respect to associated Legendre functions and spherical Bessel functions. New recurrence relationships are found for calculating the fields in the layers. They ensure high numerical efficiency of the solution. The novelty and efficiency of the proposed method are due to the form of record of the radial part of the solution, which is presented in the form of normalized functions that satisfy the condition of continuity of the Debye potentials at the layer interfaces. Analytical representations have been obtained for the components of the scattered field in the near and far diffraction zones. High accuracy and reliability of the found solution was confirmed by the analysis of the inner solution convergence and comparison with the numerical methods.

Basing on the found solution, we have analyzed the distribution of the scattered field of a plane wave by spherical lenses in the RF band. As the number of the layers, which approximate the profile of the dielectric permittivity of a lens, grows, the electric field at the focal point increases and reaches the maximum value, which allows one to determine the minimal required number of layers in practical problems. It was found that in the example under consideration, an eight-layer structure is sufficient for the development of spherical lens antennas of mobile communication base stations. The development method can be used efficiently to design and manufacture various lens antennas, as well as to study metal-dielectric structures in the optical range, e.g, nanoparticles of gold, silver, and other metals covered with dielectrics.

Analysis of the applicability limits of the quasistatic approximation for calculations of metal-dielectric nanostructures demonstrated that this approximation ensures an error of less than 3% if the ratio of the particle sizes and the wavelength is no more than 0.05. It is shown that the resonance properties of metal nanospheres are pronounced better, if they are coated with dielectric sheaths having high refractive indices.

REFERENCES

1. P. O. Afanasyev, M. B. Manuilov, S. M. Matytsin, and V. A. Sledkov, *Antenny*, 3, 16 (2015).
2. A. I. Skorodumov, *Multichannel antenna systems for new-generation mobile communication with op-*

timal space frequency filtering [in Russian]: Doct. Sci. Theses, Moscow Aviation Inst. (State Techn. Univ.), Moscow (2010).

3. V. A. Kaloshin, in: *13th Intern. Crimean Conf. "Microwave Engineering and Telecommunication Technologies" (KryMiCo-2003), September 18–12, 2003, Sevastopol, Ukraine*, p. 387.
4. R. A. Shore, *IEEE Antennas and Propag. Magazine*, **57**, No. 6, 69 (2015).
5. S. P. Morgan, *IRE Transactions Antennas Propag.*, **7**, No. 4, 342 (1959).
6. V. A. Kaloshin, *Radiotekh. Élektron.*, 1, 26 (1973).
7. V. A. Kaloshin and A. S. Venetsky, in: *7th Intern. Conf. Mathematical Methods in Electromagnetic Theory (MMET), 2–5 June 1998, Kharkov, Ukraine*, p. 157.
8. J. R. Sanford, *Spherically stratified microwave lenses: Ph.D. Thesis*, Ecole Polytechnique Federale de Lausanne, Lausanne, 1992.
9. J. A. Lock, *J. Opt. Soc. America A*, **25**, No. 12, 2971 (2008).
10. E. Braun, *IRE Transactions on Antennas and Propagation*, **4**, No. 2, 132 (1956).
11. T. A. Rhys, *IEEE Transactions on Antennas Propagat.*, **18**, No. 4, 497 (1970).
12. E. G. Zelkin and R. A. Petrova, *Lens Antennas* [in Russian], Sov. Radio, Moscow (1974).
13. A. S. Venetsky and V. A. Kaloshin, *Zhurn. Radioélektron.*, 5, Art. no. 3 (2008).
14. B. Schoenlinner, X. Wu, J. P. Ebling, et al., *IEEE Trans. Microwave Theory and Techniques*, **50**, No. 9, 2166 (2002).
15. C. A. Fernandes, *IEEE Antennas and Propagation Magazine*, **41**, No. 5, 141 (1999).
16. W. C. Chew, *Waves and Fields in Inhomogeneous Media*, Van Nostrand Reinhold, New York (1990).
17. N. A. Logan, *Proc. IEEE*, **53**, No. 8, 773 (1965).
18. M. Born and E. Wolf, *Principles of Optics*, Cambridge Univ. Press (1999).
19. G. Mie, *Annalen der Physik*, **330**, No. 3, 377 (1908).
20. W. Hergert and T. Wriedt, *The Mie Theory: Basics and Applications. Springer Series in Optical Sciences*. Springer, Berlin (2012).
21. P. Debye, *Annalen der Physik*, **335**, No. 11, 57 (1909).
22. A. L. Aden and M. Kerker, *J. Appl. Phys.*, **22**, No. 10, 1242 (1951).
23. J. R. Wait, *Applied Scientific Research B*, **10**, No. 5–6, 441 (1962).
24. Z. S. Wu and Y. P. Wang, *Radio Science*, **26**, No. 6, 1393 (1991).
25. J. A. Stratton, *Electromagnetic Theory*, McGraw-Hill, New York (1941).
26. R. F. Harrington, *Time-harmonic electromagnetic fields*, McGraw-Hill, New York (1961).
27. J. Mikulski and E. L. Murphy, *IEEE Trans. Anten. Propag.*, **11**, No. 2, 169 (1963).
28. H. Mieras, *IEEE Trans. Anten. Propag.*, **30**, No. 6, 1221 (1982).
29. S. Vinogradov, E. Vinogradova, and P. Smith, in: *Intern. Conf. Electromagnetics in Advanced Applications, September, 15–17, 1999, Torino, Italy*, p. 277.
30. L.-W. Li, P.-S. Kooi, M.-S. Leong, et al., *IEEE Trans. Microwave Theory and Techniques*, **42**, No. 12, 2302 (1994).
31. E. V. Komarova, *Antenna and Diffraction Properties of the Multilayer Luneberg Lens [in Russian]. Cand. Tech. Sci. Theses*, Urals Federal Univ., Ekaterinburg (2012).
32. J. R. Sanford, *IEEE Trans. Anten. Propag.*, **42**, No. 5, 690 (1994).

33. B. Fuchs, S. Palud, L. Le Coq, et al., *IEEE Trans. Anten. Propag.*, **56**, No. 2, 450 (2008).
34. S. Rondineau, A. I. Nosich, D. Jean-Pierre, et al., *IEEE Trans. Anten. Propag.*, **52**, No. 5, 1270 (2004).
35. V. V. Akhiyarov, *Zhurn. Radioélektron.*, 12, Art. no. 13 (2015).
36. A. Lerer, I. Donets, and S. Bryzgalo, *J. Electromagnetic Waves and Applications*, **10**, No. 6, 765 (1996).
37. G. Godi, R. Sauleau, and D. Thouroude, *IEEE Trans. Anten. Propag.*, **53**, No. 4, 1278 (2005).
38. A. D. Greenwood and J.-M. Jin, *IEEE Trans. Anten. Propag.*, **47**, No. 8, 1260 (1999).
39. D. P. Zoric, D. I. Olcan, and B. M. Kolundzija, in: *2012 Intern. Symposium on Antennas and Propag. (ISAP), October 29–November 2, 2012, Nagoya, Japan*, p. 918.
40. Z. Sipus, N. Burum, and J. Bartolic, *Microwave and Optic. Techn. Lett.*, **36**, No. 4, 276 (2003).
41. V. V. Klimov, *Nanoplasmonics* [in Russian], Fizmatlit, Moscow (2009).
42. S. Peng, J. M. McMahon, G. C. Schatz, et al., *Proc. Nath. Acad. Sci. USA*, **107**, No. 33, 14530 (2010).
43. P. K. Jain, K. S. Lee, I. H. el-Sayed, and M. A. el-Sayed, *J. Phys. Chem. B*, **110**, 7238 (2006).
44. *EMSS FEKO*, https://altairhyperworks.com/product/FEKO .
45. http://www.luxpop.com .
46. B. Fuchs, L. le Coq, O. Lafond, and S. Rondineau, *IEEE Trans. Anten. Propag.*, **55**, No. 2, 283 (2007).